Anti-HIV Agents That Selectively Target Retroviral Nucleocapsid Protein Zinc Fingers without Affecting Cellular Zinc Finger Proteins†

Mingjun Huang,‡ Andrew Maynard,§ Jim A. Turpin,‡ Lisa Graham,‡ George M. Janini,|| David G. Covell,§ and William G. Rice*,‡

Laboratory of Antiviral Drug Mechanisms, Laboratory of Experimental and Computational Biology, and Chemical Synthesis and Analysis Laboratory, National Cancer Institute-Frederick Cancer Research and Development Center, SAIC Frederick, Frederick, Maryland 21702-1201

Received December 22, 1997

Agents that target the two highly conserved Zn fingers of the human immunodeficiency virus (HIV) nucleocapsid p7 (NCp7) protein are under development as antivirals. These agents covalently modify Zn-coordinating cysteine thiolates of the fingers, causing Zn ejection, loss of native protein structure and nucleic acid binding capacity, and disruption of virus replication. Concentrations of three antiviral agents that promoted in vitro Zn ejection from NCp7 and inhibited HIV replication did not impact the functions of cellular Zn finger proteins, including poly(ADP-ribose) polymerase and the Sp1 and GATA-1 transcription factors, nor did the compounds inhibit HeLa nuclear extract mediated transcription. Selectivity of interactions of these agents with NCp7 was supported by molecular modeling analysis which (1) identified a common saddle-shaped nucleophilic region on the surfaces of both NCp7 Zn fingers, (2) indicated a strong correspondence between computationally docked positions for the agents tested and overlap of frontier orbitals within the nucleophilic loci of the NCp7 Zn fingers, and (3) revealed selective steric exclusion of the agents from the core of the GATA-1 Zn finger. Further modeling analysis suggests that the thiolate of Cys49 in the carboxy-terminal finger is the site most susceptible to electrophilic attack. These data provide the first experimental evidence and rationale for antiviral agents that selectively target retroviral nucleocapsid protein Zn fingers.

Introduction

Although treatment of HIV-1 infection with multidrug therapy using a panel of recently approved potent inhibitors of HIV-1 reverse transcriptase and protease enzymes has delayed disease onset (AIDS) and death associated with HIV infection, it is now clear that these cocktails can fail for a number of reasons.[1−3] Thus, there is a clear need for the development of new antiviral agents that affect unique targets, but which do not demonstrate cross-resistance with existing drugs. In this regard, the two retroviral Zn finger motifs of the HIV-1 nucleocapsid p7 (NCp7) protein represent attractive antiviral targets. The spacing and metal-chelating residues (3 Cys, 1 His) of the Cys-X_2-Cys-X_4-His-X_4-Cys (CCHC) Zn fingers are absolutely conserved among all known retroviruses.[4−8] These CCHC Zn fingers are required for the selection and packaging of viral genomic RNA[9−12] and are implicated in a multiplicity of other events required for infection.[13]

We recently identified a series of chemotypes that target the NCp7 by chemically modifying the nucleophilic sulfur atoms of the Zn-coordinating Cys residues in the two CCHC Zn fingers, resulting in ejection of Zn.[14−20] These chemotypes include 3-nitrosobenzamide (NOBA), disulfide benzamides (DIBAs or 2,2′-dithiobisbenzamides), dithiaheterocyclic molecules such as 1,2-dithiane-4,5-diol, 1,1-dioxide, cis (dithiane), α-carbonyl azoic compounds such as azodicarbonamide (ADA), and others. Such agents have inhibited all strains of retroviruses tested[16,18,19] except the spumaretroviruses that contain no CCHC Zn fingers.[21] The agents also inactivated cell-free virions[22] and inhibited production of infectious virus from chronically infected cells.[23] To date, no resistant virus strains have been observed in cell culture with these agents. Moreover, a benzoisothiazolone derivative of the DIBA-4 compound[16] is currently in clinical trials in the United States,[24] and ADA[18] is being evaluated clinically in Europe with patients having advanced AIDS.[25]

A major point of contention in the usage of nucleocapsid protein Zn fingers as targets for intervention in the therapeutic treatment of HIV-1 infection has been the question of selectivity of the agents. The presence of Zn finger domains in normal cellular proteins has cast doubt as to whether agents can be developed that target the CCHC Zn fingers of NCp7 without affecting cellular Zn finger proteins. Herein we provide the first experimental evidence that antiviral agents can selectively

* Corresponding author: William G. Rice, Ph.D., Sr. Scientist and Head, Laboratory of Antiviral Drug Mechanisms, National Cancer Institute-Frederick Cancer Research and Development Center, SAIC Frederick, Building 431T-B, P.O. Box B, Frederick, MD 21702-1201; phone (301) 846-5060; fax (301) 846-6846; e-mail rice@dtpax2.ncifcrf.gov.

† Abbreviations: CCHC, Cys-X_2-Cys-X_4-His-X_4-Cys; NCp7, nucleocapsid p7 protein; NOBA, 3-nitrosobenzamide; DIBA, benzamide disulfides or 2,2′-dithiobisbenzamides; dithiane, 1,2-dithiane-4,5-diol, 1,1-dioxide, cis; ADA, azodicarbonamide; HIV-1, human immunodeficiency virus, type 1; PARP, poly(ADP-ribose) polymerase (EC 2.4.2.30); TSQ, *N*-(6-methoxy-8-quinolyl-)-*p*-toluenesulfonamide; AIDS, acquired immune deficiency syndrome; CZE, capillary zonal electrophoresis; DFT, density functional theory; LUMO, lowest unoccupied molecular orbital; HOMO, highest occupied molecular orbital; EC_{50}, concentration providing 50% cytoprotection; CC_{50}, concentration eliciting 50% cell death.

‡ Laboratory of Antiviral Drug Mechanisms.
§ Laboratory of Experimental and Computational Biology.
|| Chemical Synthesis and Analysis Laboratory.

S0022-2623(97)00854-6 CCC: $15.00
Published on Web 04/03/1998

target the NCp7 Zn fingers, and we provide a rationale for such selectivity.

Methods

Virus Replication Inhibition Assays. Measurement of anti-HIV-1 activity of experimental compounds was performed with CEM-SS cells and HIV-1_{RF} using the XTT cytoprotection assay as previously described.[26,27] The experimental agents were derived from the NCI chemical repository. NOBA was synthesized and provided by Octamer Research Foundation, Inc. (Mill Valley, CA), and DIBA-1 was synthesized by Parke-Davis Pharmaceuticals (Ann Arbor, MI).

Expression and Purification of NCp7 Protein. An *Escherichia coli* strain BL21 (DE3) harboring pET3a-NCp7 was a kind gift from R. De Guzman and M. F. Summers. Details for expression and purification of NCp7 protein will be published elsewhere.

HIV-1 NCp7 Zn Finger Assays. (1) TSQ Assay. The Zn selective fluorescent probe *N*-(6-methoxy-8-quinolyl-)-*p*-toluenesulfonamide (TSQ, Molecular Probes, Eugene, OR) was utilized to measure Zn released from the NCp7 protein in vitro as previously described.[17] **(2) Capillary Zone Electrophoresis (CZE).** CZE analyses were performed with a Beckman P/ACE 5500 instrument as previously described.[28] Briefly, 0.675 nmol of NCp7 (in 10 mM sodium phosphate buffer, pH 7.0) were treated with 5 nmol of each agent, mixed, incubated for 30 min at 20 °C, and resolved on a 10% linear polyacrylamide-coated fused silica column. Spectroscopic evaluations (mAU) were measured at 214 nm. **(3) Gel Shift Assay of NCp7 and ψ Oligonucleotide.** NCp7 protein (50 nM) was treated with or without experimental agents for 1 h at room temperature in 10 μL of buffer containing 10% glycerol and 50 mM Tris-HCl (pH 7.5). Thereafter, a ^{32}P-labeled 44-mer DNA-based oligonucleotide analogous to the HIV-1 ψ RNA sequence (0.1 pmol) in an equal volume buffer containing 10% glycerol, 50 mM Tris-HCl (pH 7.5), 400 mM KCl, and 40 mM $MgCl_2$ was added. The reaction was continued at room temperature for another 15 min, and 5 μL of reaction mixture was loaded onto 4.5% nondenaturing polyacrylamide gels in 0.5X Tris-borate (TBE) electrophoresis buffer after pre-electrophoresis at 150 V at 4 °C for 1 h. Products were then electrophoresed under the same conditions for 2 h, and gels were dried and analyzed by autoradiography on X-Omat AR film (Kodak, Rochester, NY).

Poly(ADP-ribose) Polymerase (PARP) Assay. The assay was performed using a kit purchased from Trevigen (Gaithersburg, MD) with modifications. The reaction mixtures were incubated at room temperature for 15 min in a 50 μL volume containing 1X reaction buffer supplied in the kit, 1 μg of activated DNA, 100 μM NAD, 5 μCi of [^{32}P]NAD (30 Ci/mmol, 2 mCi/ml), 33 μL of PARP enzyme (specific activity: 200 (pmol/min)/μL), and the test agents at various concentrations. Reactions were terminated by addition of 1 mL of ice-cold 20% trichloroacetate. The entire contents of the reaction were filtered through a GF/C filter (Whatman, Clifton, NJ) under vacuum. Filters were then washed with 10 mL of 70% ethanol and allowed to air-dry, and ^{32}P incorporation was quantitated by β-scintillation.

In Vitro Transcription Assay. The pUC119.CMV.DHBV plasmid, which contains a cytomegalovirus (CMV) immediate-early promoter and reporter sequences encoding the duck hepatitis B virus pregenome,[29] was cleaved at a Bgl II site (~700 bp downstream of the CMV promotor) and utilized as a template for in vitro runoff transcription. HeLa cell nuclear extract was obtained from Promega (Madison, WI), and in vitro transcription reactions were performed according to the manufacture's instructions, except that [^{32}P]UTP (800 Ci/mmol, 10 mCi/mL) rather than [^{32}P]GTP was used as the radiolabeled ribonucleotide. The reaction products were denatured and subjected to electrophoresis in 5% polyacrylamide gels containing 8 M urea.

Super Gel Shifting Assays. The Sp1 consensus oligonucleotide (5′ GATCGATCGGGGCGGGGCGATC 3′) and Oct-1 consensus oligonucleotide (5′ GATCGAATGCAAATCACTAGCT 3′) were purchased from Stratagene (La Jolla, CA). The GATA-1 consensus oligonucleotide (5′ CACTTGATAACA-GAAAGTGATAACTCT 3′), K562 nuclear extract and antibodies for Sp1(Sp1[PEP 2]-G), GATA-1 (GATA-1[N1]), and Oct-1 (Oct-1[C21]) were purchased from Santa Cruz Biotechnology, Inc. (Santa Cruz, CA). The binding reactions of oligonucleotides with K562 nuclear extract, as well as the electrophoretic conditions, were performed according to the procedure described in Gelshift Buffer Kit purchased from Stratagene (La Jolla, CA). Gels were dried and then exposed on X-Omat AR film (Kodak, Rochester, NY).

Molecular Modeling. Modeling studies of the NCp7 Zn finger domains were based on the NMR structure of Summers et al.[30] Docking studies treated this structure as a rigid target. The ligand conformations used in the docking procedure were obtained by sampling the lowest energy geometries from successive in vacuo molecular dynamics and minimization simulations based on the CVFF force field within Discover95.0 (Biosym/Molecular Simulation Inc., San Diego, CA). The lowest energy conformer of each ligand was subsequently HF/STO-3G optimized using Gaussian-94.[31] All heavy-atom internal coordinates were optimized; internal phenyl ring and hydrogen coordinates were constrained at their CVFF minima. Using our previously developed docking methods,[32,33] each of the optimized configurations were docked against the amino-terminal (finger 1) and carboxyl-terminal (finger 2) Zn fingers of NCp7, yielding a family of docked conformations ranked according to their computationally predicted free-energy of binding. This procedure treats the ligands and targets as rigid molecules, thus excluding the possibility of additional ligand or target flexibility (molecular dynamics) associated with interactions between molecules.

Density functional theory (DFT) calculations[34] using Dmol3.0 (Biosym/Molecular Simulation Inc., San Diego, CA) with the VWN functional and an augmented DNP basis set provided high-quality electronic structures for the ligands and NCp7 Zn finger target. Ligand geometries were the same as those used in the docking procedure. The NMR structure of the 56-atom $[Zn(CCHC)]^{-1}$ coordination complex was used to determine frontier orbitals for each Zn finger unit. The molecular orbital overlap between the lowest unoccupied molecular orbital (LUMO) of each ligand and highest occupied molecular orbital (HOMO) of the respective Zn fingers, $\langle\psi_{ligand,LUMO}|\psi_{NCp7,HOMO}\rangle$, was computed by MO transformation to the docked reference frame and application of 3D spline interpolation and quadrature.[35] Regional reactivity of the NCp7 Zn fingers was based on computation of the Fukui function,[36] $f(\boldsymbol{r})^- = (\Delta\rho/\Delta N)$, where $\Delta\rho$ is the response of the electron density to electron donation ($\Delta N = -1$) in the case of electrophilic attack. This function was considered a more robust measure of the Zn finger reactivity than the HOMO electron density due to explicit inclusion of relaxation effects from electron donation. The Fukui function was also computed using larger portions of the Zn finger domains. Finger 1 calculations used a 186-atom fragment involving residues Lys14−Pro31 and Finger 2 was based on a 174-atom fragment involving residues Gly35−Thr50. To make the calculations tractable, residues with distant side chains were converted to glycine. Hirshfeld[37] electron population analysis provided a stable means of atomic indexing $f(\boldsymbol{r})^-$ and mapping of the reactivity spectrum. Modeling of GATA-1 was based on the NMR structure of Omichinski et al.[38] The molecular docking and DFT methodologies used in the GATA-1 calculations were identical to that of NCp7. Residues Lys1−Ser60 defined the Zn finger domain of GATA-1 used in the docking analysis. Since Arg47 interacts ionically with three of the coordinated thiolates, the local electronic structure of the Zn finger was modeled as $[Zn(CCCC)R]^{-1}$.

Results and Discussion

Selection and Anti-HIV-1 Activity of NCp7 Zn Finger Inhibitors. Among the numerous compounds previously identified that inhibit HIV-1 replication by targeting the NCp7 Zn fingers, four prototypical agents

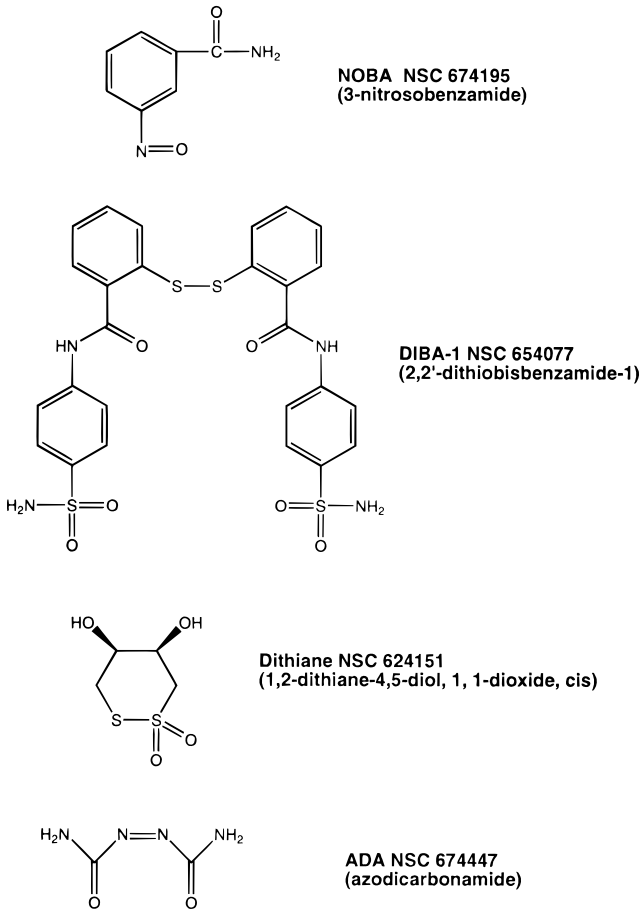

Figure 1. Structures of selected antiviral agents that target the NCp7 protein Zn fingers.

Table 1. Anti-HIV-1 Activities of NCp7 Zn Finger Inhibitors

	XTT cytoprotection assay[a]		
compound	EC_{50} (μM)	CC_{50} (μM)	TI_{50}
NOBA	–[b]	10.6	–
DIBA-1	2.3	>200	>87
dithiane	6.6	184	27.9
ADA	38	>200	>5.3

[a] The antiviral assay was performed with CEM-SS cells and HIV-1_{RF} using the tetrazolium dye 2,3-bis(methoxy-4-nitro-5-sulfophenyl)carbonyl]-2*H*-tetrazolium *S*-carboxanilide salt (XTT) to quantitate the ability of a compound to prevent HIV-induced cytopathicity. EC_{50} indicates the drug concentration that provides 50% cytoprotection and the CC_{50} reflects the drug concentration that elicits 50% cell death. [b] Due to toxicity to the CEM-SS cells by NOBA, no EC_{50} could be obtained.

representing different chemotypes were selected for study. These include NOBA as a representative of C-nitroso compounds, DIBA-1 as the representative of disulfide benzamides, dithiane as the representative of dithiaheterocyclic compounds, and ADA as the representative of the α-carbonyl azoic compounds (see Figure 1). DIBA-1, dithiane, and ADA all exerted in vitro anti-HIV-1 activity (Table 1), and the antiviral activity of these agents with various HIV-1, HIV-2, and SIV strains, as well as their lack of effects on other antiviral targets, have been published previously.[16,18,19] As reported previously,[14,15] NOBA inhibited HIV-1 replication in PBMC cultures with an $EC_{50} = 1.56$ μM (concentration providing 50% cytoprotection) and $CC_{50} = 50$ μM (concentration eliciting 50% cell death), but was unable to exert a demonstrable anti-HIV-1 effect in the XTT-based assay because of toxicity to the CEM-SS tumor cells.[39]

Reactions of the Compounds with NCp7 Protein Zinc Fingers. The ability of each of the agents to eject Zn from NCp7 in vitro was determined by TSQ assay.[17] All four agents promoted a time-dependent increase in fluorescence as Zn was ejected from NCp7 (Figure 2A), whereas other compounds such as RT inhibitors (AZT, ddI, ddC, and Nevirapine) and the KNI-272 protease inhibitor did not.[18,19] The rate of Zn ejection from NCp7 was concentration-dependent and relatively equivalent among the agents, although DIBA-1 promoted the most rapid Zn ejection. NCp7 in the absence of Zn finger reactive agents does not induce TSQ fluorescence during the time period of the assay. This is because the Zn is tightly coordinated in the CCHC Zn finger motifs,[40,41] with K_d values in the range of 10^{-2} M.

Modification of NCp7 by these agents was confirmed by capillary zone electrophoresis (CZE, Figure 2B).[28] The precise rate of migration of the NCp7 is determined by a combination of parameters, including the size, charge, and shape of the molecule. NCp7 alone formed a sharp peak at a migration time of ~9.6 min. Treatment of NCp7 with the Zn ejectors resulted in shifts in the peak position, broadening of its peak, and/or formation of multiple peaks. These complex patterns in CZE electrophoretograms reflect the formation of covalent adducts with NCp7. Unstable adducts may tend to collapse and form disulfide cross-links among Cys residues within the Zn fingers.[42,43] Moreover, the relative proportions of products depend on the concentration of agent used and the time allowed for the reaction to proceed. Although the products generated by the agents may differ, these CZE studies clearly demonstrate that these agents cause major conformational changes in the NCp7 protein.

To determine if modification of the NCp7 protein by these agents alters its ability to bind nucleic acids, we performed a gel shift assay using a 44-mer DNA oligonucleotide probe that is analogous to the HIV-1 RNA ψ packaging sequence.[44−46] Figure 2C illustrates the gel shift as a consequence of formation of an NCp7:probe complex (lane 2). After treatment of NCp7 for 1 h with NOBA or dithiane at concentrations of >1 μM, the NCp7 lost its ability to bind the probe. Treatment of NCp7 with 10 μM ADA resulted in partial inhibition of binding activity, and 100 μM ADA completely inhibited binding. Incubation of NCp7 with 1 μM of these agents for longer periods (2−3 h) resulted in complete blockage of NCp7:probe complex formation (data not shown). The effect of DIBA-1 on NCp7 binding of the probe could not be assessed due to problematic solubility properties of the compound under the buffer conditions used. However, DIBA-1 was observed to block complex formation in the 1−10 μM range under other conditions (data not shown) and previously by Tummino et al.[47] Together, these studies demonstrate the relatively equivalent abilities of the four chemotypes to promote in vitro Zn ejection from the HIV-1 NCp7 protein Zn fingers and to cause alterations in both the conformation and nucleic acid-binding properties of the protein. The concentration range of agents required for NCp7 Zn finger reactivity was also equivalent to levels that

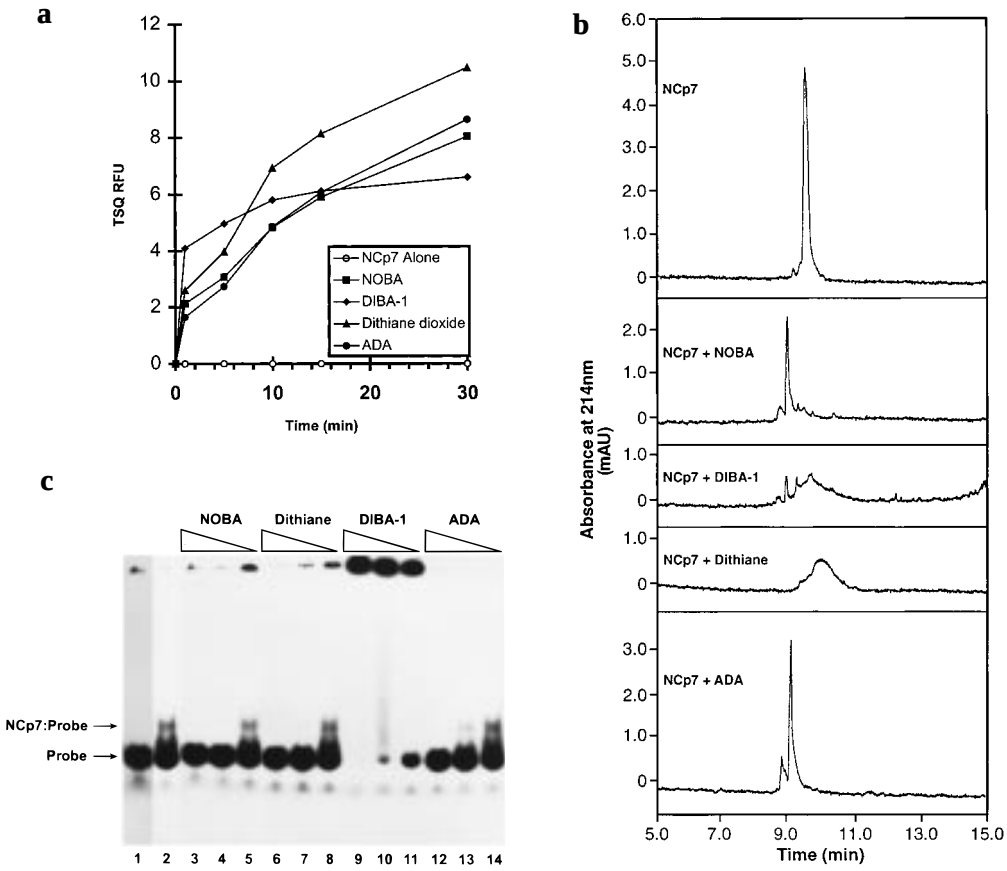

Figure 2. Reactions of agents with NCp7 protein Zn fingers. (A) TSQ assay. The Zn selective fluorescent probe TSQ was used to measure the time-dependent in vitro release of Zn from both fingers of the NCp7 protein after exposure to 10 μM concentrations of the indicated compounds. (B) CZE assay. The assay was performed as described in Methods, and modified NCp7 protein displayed alterations in mobility patterns. (C) Gel shifting assay. The assay was performed as described in Methods: lane 1, probe alone; lane 2, probe and NCp7; lanes 3−5, probe, NCp7, and NOBA; lanes 6−8, probe, NCp7, and dithiane; lanes 9−11, probe, NCp7, and DIBA-1; lanes 12−14, probe, NCp7, and ADA. Concentrations of compounds utilized were as follows: 1 μM in lanes 5, 8, 11, and 14; 10 μM in lanes 4, 7, 10, and 13; 100 μM in lanes 3, 6, 9, and 12.

elicited in vitro anti-HIV-1 effects, defining the concentration bracket of 1−100 μM for usage in subsequent studies.

Evaluation of NCp7 Zn Ejectors against the Cellular Poly(ADP-ribose) Polymerase Zn Finger Protein. Poly(ADP-ribose) polymerase (PARP), a nuclear enzyme that participates in a range of DNA rejoining activities[48−52] and apoptotic events,[39,53−57] contains two CCHC-type Zn finger motifs. However, the spacing between the metal-chelating residues are symmetrical and form longer fingerlike loops than those of the retroviral CCHC Zn fingers (see Figure 3). NOBA was previously shown to promote Zn ejection from one of the Zn fingers of PARP, resulting in inhibition of enzymatic activity.[58] We found that NOBA inhibited in vitro PARP activity with an IC_{50} = 1.8 μM (Figure 4A). However, even 100 μM of the other three agents did not significantly affect PARP, and other anti-HIV-1 drugs (AZT, ddC and KNI-272) also showed no inhibitory effect on PARP (Figure 4B). These results clearly distinguish the ability of different agents to exert discriminating reactivity between different Zn finger proteins. In addition, the findings indicate that NOBA can be used as an internal standard for different assay systems since all of the chemotypes affected NCp7 Zn fingers relatively equivalently but only NOBA affected PARP.

Evaluation of NCp7 Zn Ejectors against Cellular Zn Finger Containing Transcription Factors. Three major types of Zn-binding Cys-rich motifs have been described.[59,60] CCHC-type Zn fingers of retrovirus NC proteins and PARP are somewhat rare, while the classical type CCHH and CCCC motifs are more commonly used by cellular proteins. In particular, cellular transcription factors have adapted CCHH and CCCC Zn fingers[8] for facilitating their binding to target DNA sequences,[61,62] and three transcription factors were chosen for study. The Sp1 and GATA-1 transcription factors were selected for study because of their requirements for intact Zn fingers for their DNA binding properties are well-characterized and because specific antibodies are readily available for studying these proteins in transcriptionally competent reaction mixtures by electrophoretic mobility shift assays. Sp1 contains three classic CCHH type Zn fingers (Figure 3) that confer sequence specificity for DNA binding, and occupation of these fingers with Zn is required for functional competence of the protein.[63] GATA-1, on the other hand, uses two CCCC type Zn fingers (Figure 3) to mediate its interactions with DNA.[64] Oct-1, a nonZn finger containing transcription factor protein, was used as a control. To determine if NCp7 Zn ejectors adversely affect cellular transcription factors containing CCHH or CCCC Zn fingers, we utilized gel shifting assays, as

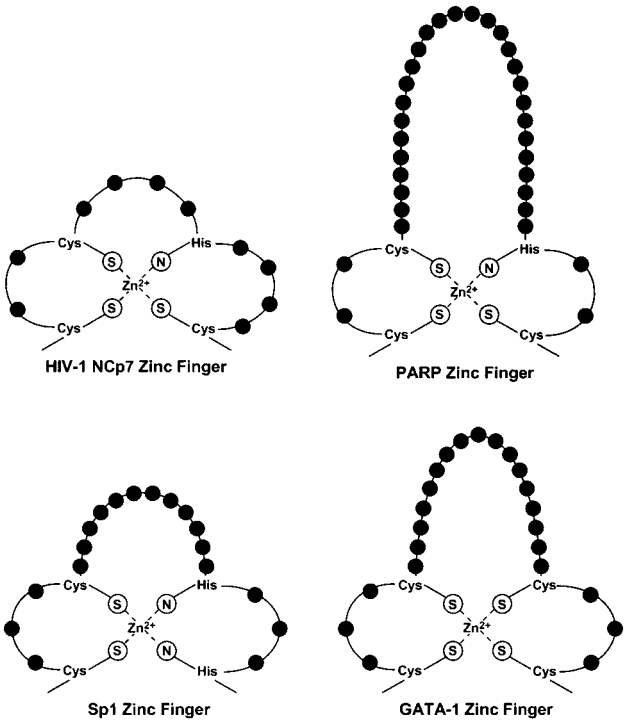

Figure 3. Zn Finger structures of HIV-1 NCp7 and selected cellular proteins. The conserved Zn fingers of HIV-1 NCp7 and the cellular PARP, Sp1 and GATA-1 proteins are depicted. Zn is coordinated via the sulfur atoms (S) of cysteine (Cys) thiolates or the nitrogen atoms (N) of histidine (His) imidazoles, and the amino acids between the Zn-coordinating residues are indicated as solid circles. HIV-1 NCp7 contains two asymmetric CCHC type Zn fingers, each composed of 14 residues and loops of 2, 4, and 4 residues. PARP also has two CCHC type Zn fingers in its amino-terminal DNA binding domain. The symmetrical Zn finger shown consists of 36 total residues; the loops consist of 2, 28, and 2 residues. Transcription factor Sp1 has three classic CCHH type symmetrical Zn fingers and the loops consist of 3, 12, and 3 residues for a total of 22 residues. GATA-1 transcription factor contains two CCCC type symmetrical Zn fingers having loops of 3, 17, and 3 residues for a total of 27 residues.

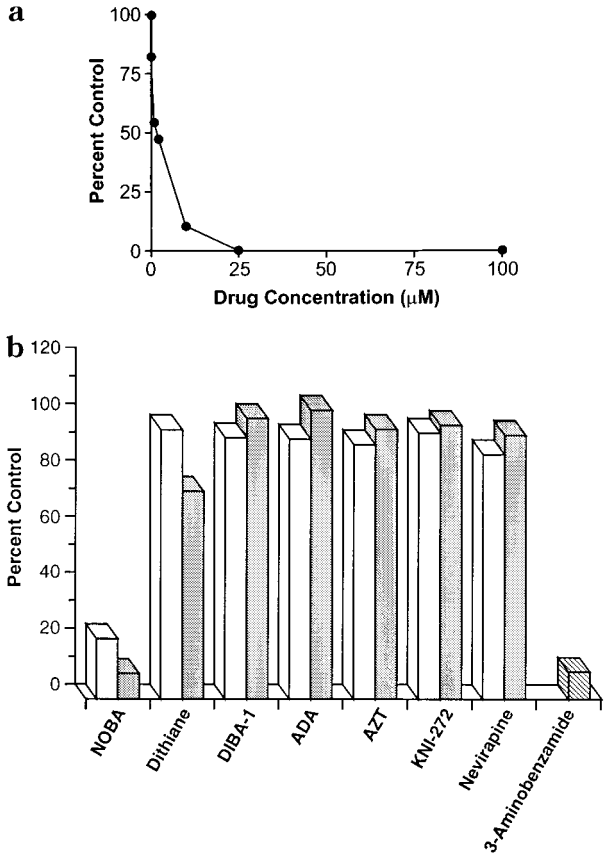

Figure 4. Effects of NCp7 Zn finger inhibitors on poly(ADP-ribose) polymerase (PARP). The effects of agents on PARP enzymatic activity were assayed using a kit purchased from Trevigen according to the manufacture's instruction, with modifications described in Methods. Panel A shows the relative PARP activity in the presence of increasing concentrations of NOBA, expressed as a percent of the control activity in the absence of compounds. Panel B shows the PARP activity in the presence of either 10 μM (open bars) or 100 μM (stippled bars) concentrations of each compound, as compared to the no drug treatment. AZT (zidovudine, nucleoside RT inhibitor), KNI-272 (protease inhibitor), and Nevirapine (nonnucleoside RT inhibitor) served as negative controls, while 3-aminobenzamide (hatched bars) is a compound included in the kit as a positive control.

was done with the NCp7 protein (see Figure 2C), to test the effects of the four agents on complex formation between transcription factors and their specific DNA recognition sequences. Since these transcription factors are contained in cellular nuclear extracts along with numerous other proteins, the specific protein:DNA complexes in question were probed with antibodies to ensure recognition of the specific complexes via super gel shifting.

As shown in Figure 5A, 100 μM NOBA caused moderate inhibition of binding of Sp1 and complete blockage of GATA-1 binding to their respective target DNA sequences, but 10 μM NOBA had no effect on either system. DIBA-1 also caused a noticeable reduction in GATA-1 binding at a concentration of 100 μM but not at 10 μM, but again the effect appeared to result from problematic solubility properties of DIBA-1. Dithiane did not significantly affect Sp1 or GATA-1 binding activities at the high test concentration of 100 μM, while 100 μM ADA caused a very modest effect only on GATA-1 binding activity. Binding of Oct-1 protein to its oligonucleotide was unaffected by all four agents. These data reinforce the prior claim that, relative to NOBA, the three other agents caused minimal to no observable changes in the DNA-binding properties of the cellular transcription factors evaluated, and none affected the nonZn finger transcription factor.

Effects of NCp7 Zn Ejectors on *in Vitro* Transcription. Because cells utilize numerous Zn finger transcription factors other than Sp1, GATA-1, and Oct-1, we examined the effects of the agents on in vitro transcription using HeLa nuclear extract as a representative source of transcription factors. In this assay, a CMV promotor was used to drive the transcription of a duck HBV pregenomic sequence. In the absence of any compounds, a runoff transcript of approximately 700 bases was readily detected (Figure 5B). NOBA completely inhibited transcript formation at concentrations of >1 μM. Dithiane caused a partial but variable inhibition only at the highest concentration of 100 μM, while DIBA-1 and ADA showed no block of transcription. These data indicate that although NOBA inhibits transcription at the same concentrations that affect PARP and other Zn finger proteins, DIBA-1, dithiane, and ADA did not significantly affect transcriptional processes.

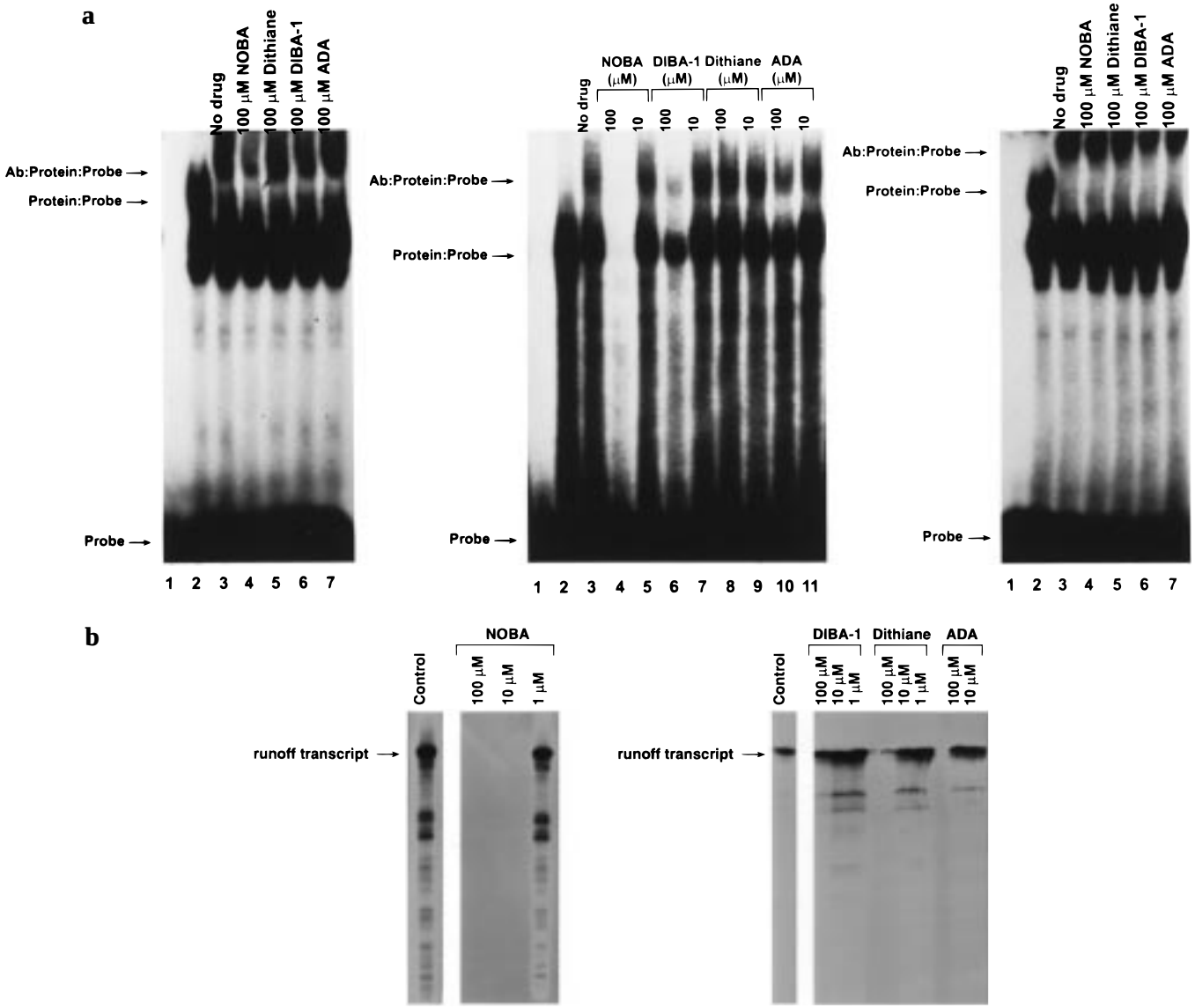

Figure 5. Effect of NCp7 Zn finger inhibitors on selected cellular transcription factors. Potential effects of compounds on cellular Zn finger proteins were assessed with super gel shifting (A) and in vitro transcription (B) assays. (A) Nuclear extract from K562 cells was incubated with [^{32}P]labeled double-stranded consensus DNA oligonucleotides (probes) to either Sp1 (left panel), GATA-1 (middle panel), or Oct-1 (right panel) in the presence of the compounds at the indicated concentrations. Following incubation, anti-Sp1 was added into reactions in lanes 3−7 of the left panel, anti-GATA-1 was added into reactions in lanes 3−11 of the middle panel, or anti-Oct-1 was added into reactions of lanes 3−7 of the right panel. The probe, protein:probe complexes, and antibody:protein:probe complexes were then resolved by nondenaturing polyacrylamide gel electrophoresis. The reaction in lane 1 of each panel did not contain nuclear extract or antibody and served as a probe only control. The reaction in lane 2 of each panel did not contain antibody and therefore served as a control for formation of protein:probe complexes in the absence of the agents. The reaction in lane 3 of each panel served as a positive control for the formation of antibody:Sp1:probe (left panel), antibody: GATA-1:probe (middle panel), or antibody:Oct-1:probe (right panel) complexes in the absence of agents. (B) In vitro transcription reactions were performed with HeLa cell nuclear extracts according to manufacture's instructions in the absence (control lane) or presence of indicated concentrations of agents. Template for runoff transcription studies was generated by cleavage of a plasmid as described in Methods. Reaction products were denatured and subjected to electrophoresis in 5% polyacrylamide gels containing 8 M urea.

Molecular Modeling of Compounds with the HIV-1 NCp7 Zn Finger Domains. The above experimental data support the conclusion that certain NCp7 zinc ejectors can interact preferentially with the Zn fingers of NCp7. To investigate this result further, we utilized molecular modeling tools to identify the most energetically favorable binding configurations of the ligands (i.e., the NOBA, DIBA-1, dithiane, and ADA antiviral agents) to both Zn fingers of the NCp7 and to further examine those docked positions for their capacity to participate in electrophilic reaction. Detailed modeling studies, such as those reported here, provide additional means of exploring the basis for the selectivity observed with biochemical procedures. It is important to acknowledge that the results of the modeling analyses are based on assumptions that necessarily simplify the true complexities of this system. Despite these limitations, molecular modeling analyses can provide additional clues about the atomic nature of selectivity and apply this information to direct the synthesis of additional reagents with enhanced selectivity.

Optimized configurations of each ligand were docked against the amino-terminal (finger 1) and carboxyl-

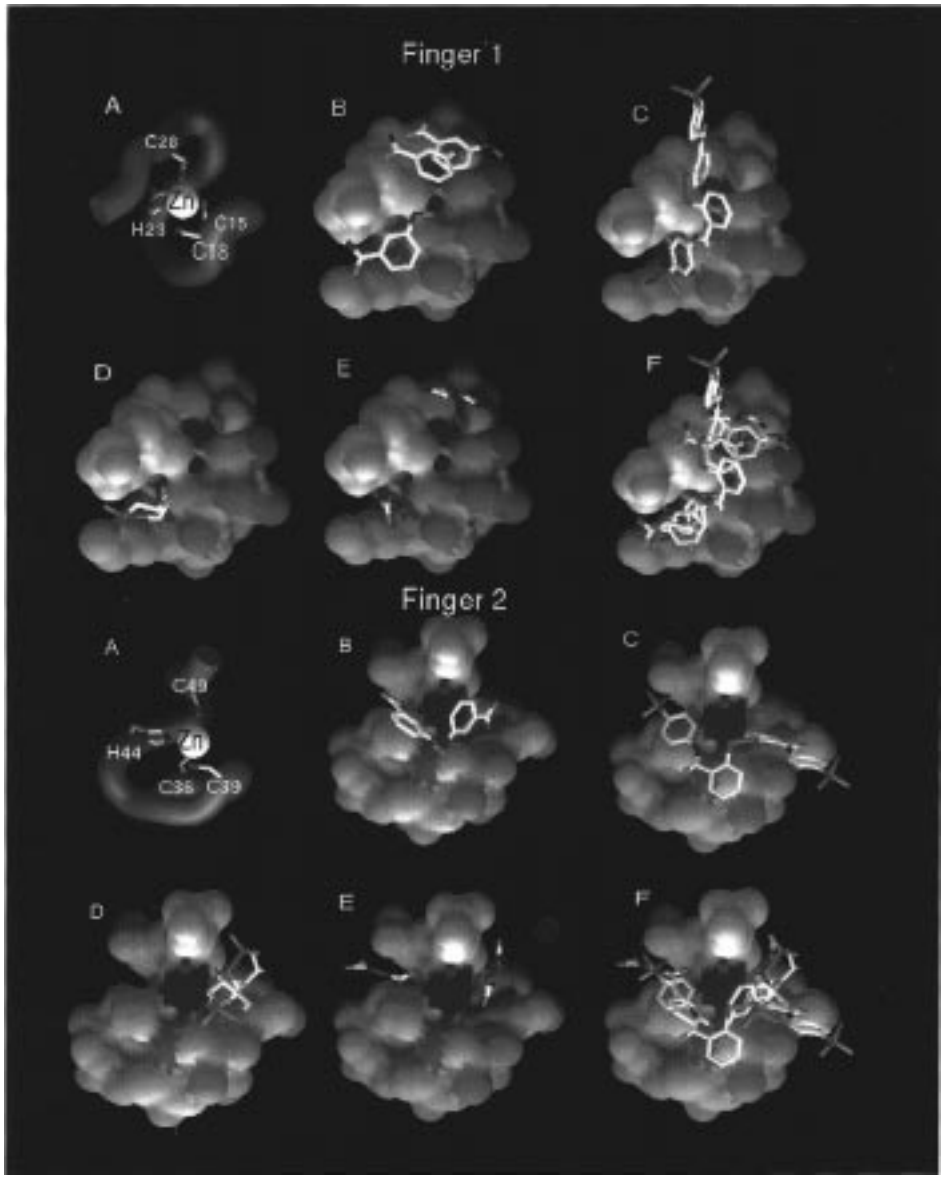

Figure 6. Docked arrangements of ligands on NCp7 Zn fingers which exhibit strong binding affinity and significant reactive molecular orbital overlap. Shown are the Connolly surfaces of each finger (0.7 Å probe radius) colored according to the atomic Fukui index; dark violet regions are the most likely sites of electrophilic attack. Upper panel, finger 1 docks from top left to bottom right: (A) finger 1 orientation indicating Zn-coordinating residues and trace of α-carbon backbone; (B) NOBA docks; (C) DIBA-1 dock; (D) dithiane docks; (E) ADA docks; (F) superposition of all docks. Lower panel, finger 2 docks from top left to bottom right: (A) finger 2 orientation indicating Zn-coordinating residues and trace of α-carbon backbone; (B) NOBA docks; (C) DIBA-1 dock; (D) dithiane docks; (E) ADA docks; (F) superposition of all docks.

terminal (finger 2) Zn fingers of NCp7, producing a nexus of docked conformations, each ranked in terms of their computationally predicted free energy of binding. Resulting docks were evaluated for their geometrical predisposition to electrophilic reaction by computing the molecular orbital (MO) overlap between the ligand LUMO and Zn finger HOMO. The HOMO−LUMO orbital set was assumed to comprise the reactive valence orbitals that drive the initial electrophilic attack on NCp7, such that enhanced overlap favors reactive covalent bond formation. Using these computational methodologies, we identified the set of docked ligands that exhibit the best theoretical scores of both binding affinity and MO overlaps that favor reaction.

The docking arrangements of each ligand are superimposed with the reactivity profiles of each Zn finger in Figure 6. Regional reactivity is displayed spectrally on the solvent-accessible surface of the Zn fingers, where dark violet indicates the most nucleophilic regions (Cys thiolates) and white the least. The reactivity spectrum corresponds to the Fukui function[36] which probes the regions of the Zn fingers most able to donate electron density and thus participate in covalent bond formation. From these calculations it is apparent that the Cys thiolates dominate the reactivity profile of NCp7. The reactive sites of finger 2 form a more contiguous reactive surface in comparison to finger 1, where they appear more isolated. The Fukui indices of thiolates S_{15} and S_{28} of finger 1 were slightly larger than S_{18}, whereas the reactivity index of S_{49} of finger 2 was significantly larger than S_{36} or S_{39}. On the basis of the sum of thiolate Fukui indices, the reactivity of finger 2 was greater than that of finger 1, the difference being the larger electronic response from S_{49}. Moreover, in

the most extensive DFT calculations, the ionization potential of finger 2 was calculated to be lower than that of finger 1. Thus, S_{49} was electronically the most nucleophilic site of the Zn fingers.

All ligands were able to dock in a manner that positioned their reactive centers adjacent to the thiolates of each Zn finger (Figure 6). The binding energies of all ligands were similar and relatively weak ($\Delta G_{bind} \approx -2$ kcal/mol). The relatively low binding energies for these complexes suggested that electrophilic approach to the Cys thiolates was dictated by steric accessibility rather than formation of a long-lived prereaction complex. The most productive binding domain of each Zn finger appeared "saddle-shaped", with two prominent "α" and "*β*" docking subdomains adjacent to the second and last thiolates of the CCHC motifs. The residues which sterically defined these subdomains are as follows. Finger 1: α (Asn_{17}, Cys_{28}−Ala_{30}, Arg_{32}), *β* (Asn_{17}, Cys_{18}, Lys_{20}, His_{23}, Pro_{31}, Arg_{32}). Finger 2: α (Lys_{38}, Cys_{39}, Lys_{41}, Met_{46}, Cys_{49}−Glu_{51}), *β* (Lys_{38}, Lys_{41}, His_{44}, Asp_{48}, Cys_{49}, Glu_{51}). NOBA, dithiane, and ADA docked into either of the two subdomains in each finger, while DIBA-1 docked in a position occupying both subdomains.

The docking configurations, relative proximities of the ligand reactive centers to the Cys thiolates, and corresponding frontier orbital overlaps, are summarized in Table 1, and coordinates of the docked configurations are available from the author upon request. From Table 1, the reactive approaches of all ligands to the cysteine thiolates were significantly closer for finger 2 compared to finger 1. This was particularly so for DIBA-1, where the reactive dock to finger 2 was nearly 4 Å closer than for finger 1. Correspondingly, there was enhanced frontier orbital overlap of the docks to finger 2 versus finger 1. Moreover, except for the NOBA docks, S_{49} tended to be the thiolate of finger 2 in closest proximity to the ligand reactive centers. On the basis of both steric accessibility and electronic response of the NCp7 Zn fingers, these findings suggest that S_{49} is the site most susceptible to electrophilic attack. These results are consistent with the biochemical data of Hathout et al.,[43] in which the Cys49 was shown to be the preferred site for electrophilic attack by 2,2′-dithiopyridine. In a similar fashion, the *E. coli* Ada protein contains a CCCC Zn finger that is required for repair of methylphosphotriesters (MeP) after damage to DNA by alkylating agents.[65] The sulfur atom of the third Cys of the CCCC motif, and only that Cys residue, mediates a nucleophilic attack only on the methyl carbon of the MeP moiety and repairs the mutagenic lesion. Thus, precedent exists in support of our observation that individual activated sulfur atoms of Cys residues in Zn fingers can selectively participate in nucleophile:electrophile interactions.

Molecular Modeling of Compounds with the GATA-1 CCCC Zn Finger Domain. The reactive accessibility of the ligands with the NCp7 Zn finger thiolates was contrasted with the GATA-1 Zn finger, which represents the core of the DNA-binding domain. Using identical procedures as with the NCp7 analysis, the set of ligand docking configurations with the strongest binding affinities and MO overlaps were computed for GATA-1 (Figure 7). DFT calculations indicated that the thiolates were also the dominant nucleophilic sites

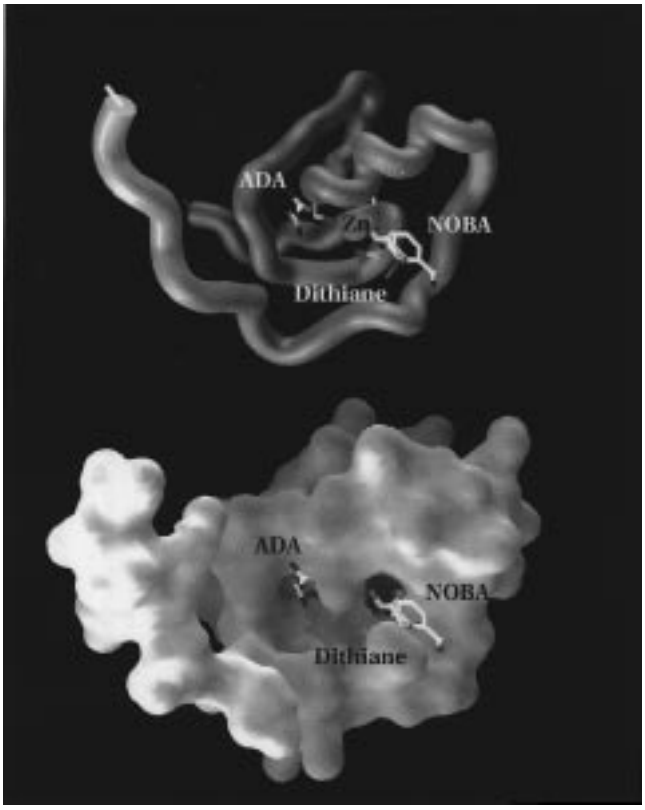

Figure 7. Docked arrangements of ligands on GATA-1 CCCC Zn fingers. The top panel displays a ribbon trace of the complete GATA-1 NMR structure. The position of the Zn atom is shown as a red sphere, with three of the four Zn-coordinating Cys side chains visible in this orientation. The best scoring docked positions for ligands ADA, dithiane, and NOBA are displayed as stick figures (color-coded as C, white; N, blue; S, green; and O, red). The bottom panel displays the molecular surface of the complete GATA-1 structure, color-coded by the local Fukui function, such that the dark violet, light violet, and white surfaces indicate the strongest (thiolates), weakest, and nonnucleophilic sites, respectively. In this figure, the nitroso group of NOBA ligand is 4.3 Å from thiolate S_{31}. DIBA-1 is not shown in the figure because an appropriate docking position was not found.

of GATA-1. Moreover, the ionization potential of the GATA-1 Zn finger was significantly lower than NCp7 due to the excess electron density associated with the additional Cys thiolate of the CCCC motif. However, due to steric exclusion, the ligand approaches to the thiolates of GATA-1 were of significantly greater distances on average than the proximities of the docked ligands to the NCp7 Zn finger thiolates.

The docks most prone to reaction are reported in Table 2. NOBA, and to a much lesser extent ADA, were able to achieve docking proximities comparable to the results of NCp7. However, DIBA-1 and dithiane were not able to dock in close proximity to the GATA-1 thiolates to promote reaction. Although the docked dithiane ring superpositioned with the NOBA phenyl ring, the *S*-SO_2 sulfur did not orient toward the GATA-1 thiolates. In addition, a significant deterrant of ligand docking to the GATA-1 Zn finger was steric hindrance. Notably, Arg47 sterically hindered access of the ligands to the GATA-1 thiolates. Of these, only NOBA was able to dock such that its reactive group (N═O) was as close to S_{31} as was Arg47 (4.3 Å to S_{31}). The banana-like shape of NOBA, with its reactive tip, allowed NOBA to

Table 2. Summary of Ligand Docking Arrangements to Finger 1 or Finger 2 of NCp7 and the Zn Finger DNA-Binding Domain of GATA-1[a]

	NCp7 finger 1 docks			NCp7 finger 2 docks			GATA-1 docks	
ligand (rxn site)	sub domain[b]	thiolate proximity[c]	% overlap[d]	sub domain[b]	thiolate proximity[c]	% overlap[d]	thiolate proximity[c]	% overlap[d]
NOBA (N=O)	α	S_{28} 6.6	0.02	α	S_{39} 3.3, S_{49} 5.3	0.50	S_{10} 5.1, S_{31} 4.3	0.27
	β	S_{18} 5.5, S_{28} 5.8	0.18	*β*	S_{39} 3.4, S_{49} 5.2	0.64		
DIBA-1 (S−S)	α/*β*	S_{18} 8.2, S_{28} 9.6	0.02	α/*β*	S_{39} 4.8, S_{49} 5.5	0.33	S_{31} 9.0	0.01
dithiane (*S*-SO_2)	*β*	S_{18} 5.3	0.34	α	S_{49} 4.3	0.51	S_{10} 7.0	0.15
				β	S_{39} 5.4, S_{49} 5.2	0.79		
ADA (N=N)	α	S_{28} 4.8	0.03	α	S_{49} 4.2	0.54	S_{28} 5.2	0.05
	β	S_{18} 4.3	0.46	*β*	S_{39} 7.8, S_{49} 6.1	0.05		

[a] Data indicate the binding subdomains, the proximity of the ligand electrophilic reaction site to cysteine thiolates, and molecular orbital overlap of the best-scoring docks shown in Figure 6. [b] Docking site location. Finger 1: subdomain α (Asn_{17}, Cys_{28}−Ala_{30}, Arg_{32}), subdomain *β* (Asn_{17}, Cys_{18}, Lys_{20}, His_{23}, Pro_{31}, Arg_{32}). Finger 2: subdomain α (Lys_{38}, Cys_{39}, Lys_{41}, Met_{46}, Cys_{49}−Glu_{51}), subdomain *β* (Lys_{38}, Lys_{41}, His_{44}, Asp_{48}, Cys_{49}, Glu_{51}). [c] Cysteine thiolates (labeled by residue) in closest proximity to the indicated ligand reactive center followed by their relative distance in Å. [d] Normalized HOMO−LUMO overlaps, such that an overlap value of 1.0 is indicated as 100%.

sterically penetrate the GATA-1 Zn finger core and deliver its nitroso group in reactive proximity to the Cys thiolates. These results are consistent with the electrophoretic mobility supershift experimental findings of GATA-1 (see Figure 5), wherein NOBA extensively affected the ability of GATA-1 to associate with nucleic acids and ADA showed a modest effect only at the high test concentration of 100 μM. Thus, the computational and biochemical studies regarding selective reactivity of antiviral agents with the NCp7 Zn fingers were in high accord.

Conclusions

The nucleophilic sulfur atoms of HIV-1 NCp7 Zn fingers can be targeted for chemical modification as an antiviral strategy. DIBA-1,[16,17] dithiane,[19] ADA,[18,25] and other related NCp7 Zn ejectors can inhibit the replication of HIV-1 and other retroviruses at concentrations that do not exert cytotoxic effects, indicating a degree of selectivity of the agents for the CCHC Zn finger target of the virus. Selectivity is also seen in the fact that these compounds were found to inhibit the replication of all retroviruses tested except the spumaretroviruses that do not contain Zn fingers in their NC proteins.[21] Examination of whether these four key chemotypes can selectively target the NCp7 Zn fingers without affecting other cellular protein Zn fingers was addressed herein by both biochemical and computational approaches. We evaluated the effects of these agents on selected cellular proteins that require Zn fingers for their biochemical functions. NOBA was relatively promiscuous in its reactivity toward various Zn finger proteins, affecting poly(ADP-ribose) polymerase (PARP) activity as well as the binding of Sp1 and GATA-1 to their target DNA probes. The exact mechanisms involving Sp1 and GATA-1 are not known, but since NOBA failed to alter Oct-1 binding (a non-Zn finger containing transcription factor), it is reasonable that inhibition may be related to reactivity with the transcription factor Zn fingers. In contrast, neither DIBA-1, dithiane, nor ADA significantly affected PARP activity or altered specific binding of the transcription factors to their DNA targets. Likewise, neither DIBA-1, dithiane, nor ADA significantly altered cellular nuclear protein-mediated transcription from a CMV promoter construct, as evidenced by their failure to reduce either the quantity or types of runoff transcript products. Thus, DIBA-1, dithiane, and ADA demonstrated selective reactivity for the retroviral Cys-X_2-Cys-X_4-His-X_4-Cys Zn fingers and caused little or no overt alterations to the functions of the cellular Zn finger proteins tested.

Selectivity of these agents for the NCp7 Zn fingers depends on the interplay of multiple factors, including ligand binding affinity, ligand reactive proximity, and sufficient redox properties to drive the reaction. Molecular modeling studies suggest that the S_{49} locus of finger 2 appears to be the favored site for electrophilic attack and provide theoretical evidence for common binding pockets for the four prototypical chemotypes on the surface of NCp7 Zn fingers. The arrangements of ligands docked to NCp7, identified in Figure 6, provide a snapshot of the putative saddle-shaped domain into which the ligands could dock and promote productive electrophilic attack on Zn finger sulfur atoms. As an example of how the computational studies have predicted reactivity of ligands for the NCp7 Zn fingers, we previously reported that ADA docks efficiently to the NCp7 Zn fingers but that a dimethylamine analogue did not because the analogue could not make critical hydrogen bonds with the Zn finger backbone residues that were made by ADA.[18] Indeed, the dimethylamine analogue was found to only very poorly promote Zn ejection from the NCp7, even though the analogue possesses a redox potential sufficient to react with the Cys thiolates. In addition to illustrating the potential predictive power of the molecular modeling, the findings with the dimethylamine ADA also provide a negative control compound that adds credibility to the inherently speculative nature of modeling studies. Finally, more detailed modeling studies of the reactivity of the NCp7 Zn fingers versus the Zn fingers of other proteins are currently under investigation (Maynard, A. T.; Huang, M.; Rice, W. G.; Covell, D. G., manuscript in preparation).

It is intriguing to note that computational studies suggested differences in the docking proximities and reactivities between the two fingers of the NCp7 protein. Previous biochemical studies by Hathout et al.[43] have directly demonstrated the nonequivalency in the reactivity of the two Zn fingers. Given the bias among the reactivities of sulfur atoms within NCp7 alone, it is reasonable to expect that the reactivity of Zn fingers of other proteins may also exhibit similar differences. Such differences in reactivities may result from the

sulfur atoms of Zn fingers of other proteins being sterically excluded from reactive ligand contact by surrounding amino acid residues. This indeed was demonstrated by the modeling analysis of the Zn finger of GATA-1. Alternatively, the electronic properties of Zn-coordinating sulfur atoms in various Zn finger proteins may differentially promote reactions with various electrophilic reagents. Nevertheless, it is clear that different Zn fingers provide different functions and nucleic acid recognition patterns that can produce biases in their chemical reactivities with ligands. Thus, our findings provide both experimental and computational evidence for antiviral agents to selectively target the NCp7 Zn fingers, and these observations may be directly applicable to identifying agents reactive with other Zn finger proteins.

Acknowledgment. This research was supported in part by the National Cancer Institute, Contract N01-C0-56000. The content of this publication does not necessarily reflect the views or policies of the Department of Health and Human Services, nor does mention of trade names, commercial products or organizations imply endorsement by the U.S. government. We thank Dr. Dennis Michaels (Monoclonal Antibody and Recombinant Protein Production Facility, NCI-FCRDC, Frederick, MD) for purification of NCp7 protein, Ms. Judy Duears for assistance in preparation of the manuscript, and Ms. Terry Williams for preparation of figures.

References

(1) Cohen, J. AIDS therapies the daunting challenge of keeping HIV suppressed. *Science* **1997**, *277*, 32−33.
(2) Wong, J. K.; Hezareh, M.; Gunthard, H. F.; Havlir, D. V.; Ignacio, C. C.; Spina, C. A.; Richman, D. D. Recovery of replication-competent HIV despite prolonged suppression of plasma viremia. *Science* **1997**, *278*, 1291−1295.
(3) Finzi, D.; Hermankova, M.; Pierson, T.; Carruth, L. M.; Buck, C.; Chaisson R. E.; Quinn, T. C.; Chadwick, K.; Margolick, J.; Brookmeyer, R.; Gallant, J.; Markowitz, M.; Ho, D. D.; Richman, D. D.; Siliciano, R. F. Identification of a reservoir for HIV-1 in patients on highly active antiretroviral therapy. *Science* **1997**, *278*, 1295−1300.
(4) Berg, J. M. Potential metal-binding domains in nucleic acid binding proteins. *Science* **1986,** *232*, 485−487.
(5) Chance, M. R.; Sagi, I.; Wirt, M. D.; Frisbie, S. M.; Scheuring, E.; Chen, E.; Bess, J., Jr.; Henderson, L. E.; Arthur, L. O.; South, T. L.; Perez-Alvarado, G.; Summers, M. F. Extended x-ray absorption fine structure studies of a retrovirus: Equine infectious anemia virus cysteine arrays are coordinated to zinc. *Proc. Natl. Acad. Sci. U.S.A.* **1992**, *89*, 10041−10045.
(6) Henderson, L. E.; Copeland, T. D.; Sowder, R. C.; Smythers, G. W.; Oroszlan, S. Primary structure of the low molecular weight nucleic acid-binding proteins of murine leukemia viruses. *J. Biol. Chem.* **1981,** *256*, 8400−8406.
(7) South, T. L.; Blake, P. R.; Sowder, R. C., II.; Arthur, L. O.; Henderson, L. E.; Summers, M. F. The nucleocapsid protein isolated from HIV-1 particles binds zinc and forms retroviral-type zinc fingers. *Biochemistry* **1990**, *29*, 7786−7789.
(8) South, T. L.; Summers, M. F. Zinc fingers. *Adv. Inorg. Biochem. Ser.* **1990**, *8*, 199−248.
(9) Aldovini, A.; Young, R. A. Mutations of RNA and protein sequences involved in human immunodeficiency virus type 1 packaging result in production of noninfectious virus. *J. Virol.* **1990**, *64*, 1920−1926.
(10) Bowles, N. E.; Damay, P.; Spahr, P.-F. Effect of rearrangement and duplications of the Cys-His motifs of Rous Sarcoma virus nucleocapsid protein. *J. Virol.* **1993**, *67*, 623−631.
(11) Dorfman, T.; Luban, J.; Goff, S. P.; Haseltine, W. A.; Göttlinger, H. G. Mapping of functionally important residues of a cysteine-histidine box in the human immunodeficiency virus type 1 nucleocapsid protein. *J. Virol.* **1993**, *67*, 6159−6169.
(12) Gorelick, R. J.; Chabot, D. J.; Rein, A.; Henderson, L. E.; Arthur, L. O. The two zinc fingers in the human immunodeficiency virus type 1 nucleocapsid protein are not functionally equivalent. *J. Virol.* **1993**, *67*, 4027−4036.
(13) Darlix, J.-L.; Lapadat-Tapolsky, M.; de Rocquigny, H.; Roques, B. P. First glimpses at structure-function relationships of the nucleocapsid protein of retroviruses (review). *J. Mol. Biol.* **1995**, *254*, 523−537.
(14) Rice, W. G.; Schaeffer, C. A.; Harten, B.; Villinger, F.; South, T. L.; Summers, M. F.; Henderson, L. E.; Bess, J. W., Jr.; Arthur, L. O.; McDougal, J. S.; Orloff, S. L.; Mendeleyev, J.; Kun, E. Inhibition of HIV infectivity by zinc-ejecting *C*-nitroso compounds. *Nature* **1993**, *361*, 473−475.
(15) Rice W. G.; Schaeffer, C. A.; Graham, L.; Bu, M.; McDougal, J.; Orloff, S. L.; Villinger, F.; Young, M.; Oroszlan, S.; Fesen, M. R.; Pommier, Y.; Mendeleyev, J.; Kun, E. The site of antiviral action of 3-nitrosobenzamide on the infectivity process of human immunodeficiency virus in human lymphocytes. *Proc. Natl. Acad. Sci. U.S.A.* **1993**, *90*, 9721−9724.
(16) Rice, W. G.; Supko, J. G.; Malspeis, L.; Clanton, D. J.; Bu, M.; Graham, L.; Schaeffer, C. A.; Turpin, J. A.; Domagala, J.; Gogliotti, R.; Bader, J. P.; Halliday, S. M.; Coren, L.; Arthur, L. O.; Henderson, L. E.; Buckheit, R. W., Jr. Novel inhibitors of HIV-1 p7NC zinc fingers as candidates for the treatment of AIDS. *Science* **1995**, *270*, 1194−1197.
(17) Rice, W. G.; Turpin, J. A.; Schaeffer, C. A.; Graham, L.; Clanton, D.; Buckheit, R. W., Jr.; Zaharevitz, D.; Summers, M. F.; Wallqvist, A.; Covell, D. G. Evaluation of selected chemotypes in coupled cellular and molecular target-based screens identifies novel HIV-1 zinc finger inhibitors. *J. Med. Chem.* **1996**, *39*, 3606−3616.
(18) Rice, W. G.; Turpin, J. A.; Huang, M. J.; Clanton, D.; Buckheit, R. W., Jr.; Covell, D. G.; Wallqvist, A.; McDonnell, N.; De Guzman, R. N.; Summers, M. F.; Zalkow, L.; Bader, J. P.; Haugwitz, R. D.; Sausville, E. A. Azodicarbonamide inhibits HIV-1 replication by targeting the nucleocapsid protein. *Nat. Med.* **1997**, *3*, 341−345.
(19) Rice, W. G.; Baker, D. C.; Schaeffer, C. A.; Graham, L.; Bu, M.; Terpening, S.; Clanton, D.; Schultz, R.; Bader, J. P.; Buckheit, R. W., Jr.; Field, L.; Singh, P. K.; Turpin, J. A. Inhibition of multiple phases of human immunodeficiency virus type 1 replication by a dithiane compound that attacks the conserved zinc fingers of retroviral nucleocapsid proteins. *Antimicrob. Agents Chem.* **1997**, *41*, 419−426.
(20) Rice, W. G.; Turpin, J. Virus-encoded zinc finger as targets for antiviral chemotherapy. *Rev. Med. Virol.* **1996**, *6*, 187−199.
(21) Rein, A.; Ott, D. E.; Mirro, J.; Arthur, L. O.; Rice, W. G.; Henderson, L. E. Inactivation of murine leukemia virus by compounds that react with the zinc finger in the viral nucleocapsid protein. *J. Virol.* **1996**, *70*, 4966−4972.
(22) Turpin, J. A.; Schaeffer, C. A.; Terpening, S. J.; Graham, L.; Bu, M.; Rice, W. G. Reverse transcription of human immunodeficiency virus type 1 is blocked by retroviral zinc finger inhibitors. *Antiviral Chem. Chemother.* **1997**, *8*, 60−69.
(23) Turpin, J. A.; Terpening, S. J.; Schaeffer, C. A.; Yu, G.; Glover, C. J.; Felsted, R. L.; Sausville, E. A.; Rice, W. G. Inhibitors of HIV-1 zinc fingers prevent normal processing of Gag precursors and result in the release of noninfectious virus particles. *J. Virol.* **1996**, *70*, 6180−6189.
(24) Domagala, J. M.; Bader, J. P.; Gogliotti, R. D.; Sanchez, J. P.; Stier, M. A.; Song, Y.; Vara Prasad, J. V. N.; Tummino, P. J.; Scholten, J.; Harvey, P.; Holler, T.; Gracheck, S.; Hupe, D.; Rice, W. G.; Schultz, R. A new class of anti-HIV-1 agents targeted toward the nucleocapsid protein NCp7: the 2,2′-dithiobisbenzamides. *Bioorg. Med. Chem.* **1997**, *5*, 569−579.
(25) Vandevelde, M.; Witvrouw, M.; Schmit, J. C.; Sprecher, S.; De Clercq, E.; Tassignon, J. P. ADA, a potential anti-HIV drug. *AIDS Res. Hum. Retrovir.* **1996**, *12*, 567−568.
(26) Weislow, O. S.; Kiser, R.; Fine, D. L.; Bader, J.; Shoemaker, R. H.; Boyd, M. R. New soluble-formazan assay for HIV-1 cytopathic effects: application to high-flux screening of synthetic and natural products for AIDS-antiviral activity. *J. Natl. Cancer Inst.* **1989**, *81*, 577−586.
(27) Rice, W. G.; Bader, J. P. In *Discovery and in Vitro development of AIDS antiviral drugs as biopharmaceuticals*; August, J. T., Anders, M. W., Murad, F., Coyle, J. T., Eds.; Academic Press: San Diego, 1995; Vol. 33, pp 389−438.
(28) Janini, G. M.; Fisher, R. J.; Henderson, L. E.; Issaq, H. J. Application of capillary zone electrophoresis for the analysis of proteins, protein-small molecules, and protein-DNA interactions. *J. Liq. Chromatogr.* **1995**, *18*, 3617−3628.
(29) Summers, J.; Smith, P. M.; Huang, M.; Yu, M. Morphogenetic and regulatory effects of mutations in the envelope proteins of an avian hepadnavirus. *J. Virol.* **1991**, *65*, 1310−1317.
(30) Summers, M. F.; Henderson, L. E.; Chance, M. R.; Bess, J. W., Jr.; South, T. L.; Blake, P. R.; Perez-Alvarado, G.; Sowder, R. C.; Hare, D. R.; Arthur, L. O. Nucleocapsid zinc fingers detected in retroviruses: EXAFS studies of intact viruses and the solution-state structure of the nucleocapsid protein from HIV-1. *Protein Sci.* **1992,** *1*, 563−574.
(31) Frish, M. J.; et al. Gaussian 94, Rev. C.3, Gaussian Inc., Pittsburgh, PA, 1995.

(32) Wallqvist, A.; Junigan, R.; Covell, D. G. A preference-based free-energy parameterization of enzyme-inhibitor binding. Applications to HIV-1-protease inhibitor design. *Protein Sci.* **1995,** *4*, 1881−1903.
(33) Wallqvist, A.; Covell, D. G. Docking enzyme-inhibitor complexes using a preference based free-energy surface. *Proteins: Struct., Funct., Genet.* **1996,** *25*, 403−419.
(34) Delley, B. In *Dmol, a Standard Tool for Density Functional Calculation: Review and Advances;* Seminario, J., Politzer, P., Eds.; (Elsevier Science B.V.: Amsterdam, 1995; pp 221−254.
(35) Press, W. H.; Flannery, B. P.; Tinkolsky, S. A.; Vetterling, W. T. *Numerical Recipes*; Cambridge University Press: Cambridge, 1986.
(36) Parr, R. G.; Yang, W. In *Density-Functional Theory of Atoms and Molecules*; International series of Monographs on Chemistry; Breslow, R., Goodenough, J. B., Halpern, J., Rowlinson, J. S., Eds.; Oxford Science Publications; Oxford, 1989; Vol. 16, pp 87−101 and 218−234.
(37) Hirshfeld, F. L. Bonded atom fragments for describing molecular charge densities. *Theor. Chim. Acta B* **1977**, *44*, 129−138.
(38) Omichinski, J. G.; Marius Clore, G.; Schaad, O.; Felsenfeld, G.; Trainor C.; Appella, E.; Stahl, S. J.; Gronenborn, A. M. NMR structure of a specific DNA complex of Zn-containing DNA binding domain of GATA-1. *Science* **1993**, 261, 438−446.
(39) Rice, W. G.; Hillyer, C. D.; Harten, B.; Schaeffer, C. A.; Dorminy, M.; Lackey, D. A.; Kirsten, E.; Mendeleyev, J.; Buki, K.; Kun, E. Induction of endonuclease-mediated apoptosis in tumor cells by *C*-nitroso substituted ligand of poly (ADP-ribose) polymerase. *Proc. Natl. Acad. Sci. U.S.A.* **1992**, *89*, 7703−7707.
(40) Green, L. M.; Berg, J. M. A retroviral Cys-Xaa2-Cys-Xaa4-His-Xaa4-Cys peptide binds metal ions: Spectroscopic studies and a proposed three-dimensional structure. *Proc. Natl. Acad. Sci. U.S.A.* **1989,** *86*, 4047−4051.
(41) Green, L. M.; Berg, J. M. Retroviral nucleocapsid protein-metal ion interactions: Folding and sequence variants. *Proc. Natl. Acad. Sci. U.S.A.* **1990,** *87*, 6403−6407.
(42) Yu, X.; Hathout Y.; Fenselau, C.; Sowder, R. C., II; Henderson, L. E.; Rice, W. G.; Mendeleyev, J.; Kun, E. Specific disulfide formation in the oxidation of HIV-1 zinc finger protein nucleocapsid p7. *Chem. Res. Toxicol.* **1995**, *8*, 586−590.
(43) Hathout, Y.; Fabris, D.; Han, M. S.; Sowder, R. C., II.; Henderson, L. E.; Fenselau, C. Characterization of intermediates in the oxidation of zinc fingers in human immunodeficiency virus type 1 nucleocapsid protein p7. *Drug Metab. Dispos.* **1996**, *24*, 1395−1400.
(44) Priel, E.; Aflalo, E.; Seri, I.; Henderson, L. E.; Arthur, L. O.; Aboud, M.; Segal, S.; Blair, D. G. DNA binding properties of the zinc-bound and zinc-free HIV nucleocapsid protein: supercoiled DNA unwinding and DNA-protein cleavable complex formation. *FEBS Lett.* **1995**, *362*, 59−64.
(45) Dannull, J.; Surovoy, A.; Jung, G.; Moelling, K. Specific binding of HIV-1 nucleocapsid protein to PSA RNA in vitro requires N-terminal zinc finger and flanking basic amino acid residues. *EMBO J.* **1994**, *13*, 1525−1533.
(46) Berglund, J. A.; Charpentier, B.; Rosbash, M. A high affinity binding site for the HIV-1 nucleocapsid protein. *Nucleic Acids Res.* **1997**, *25*, 1042−1049.
(47) Tummino, P. J.; Scholten, J. D.; Harvey, P. J.; Holler, T. P.; Maloney, L.; Gogliotti, R.; Domagala, J.; Hupe, D. The in vitro ejection of zinc from human immunodeficiency virus (HIV) type 1 nucleocapsid protein by disulfide benzamides with cellular anti-HIV activity. *Proc. Natl. Acad. Sci. U.S.A.* **1996**, *93*, 969−973.
(48) Berger, N. A.; Petzold, S. J.; Berger, S. J. Association of poly-(ADP-rib) synthesis with cessation of DNA synthesis and DNA fragmentation. *Biochim. Biophys. Acta* **1979**, *564*, 90−104.
(49) Jacobson, M. K.; Jacobson, E. L. *ADP-ribose transfer reactions, mechanisms and biological significance*, 1st ed.; Springer-Verlag: New York, 1989.
(50) Satoh, M. S.; Lindahl, T. Role of poly(ADP-ribose) formation in DNA repair. *Nature* **1992**, *356*, 356−358.
(51) Satoh, M. S. NAD(+)-dependent repair of damaged DNA by human cell extracts. *J. Biol. Chem.* **1993**, *268*, 5480−5487.
(52) Smulson, M.; Istock, N.; Ding, R.; Cherney, B. Deletion mutants of poly(ADP-ribose) polymerase support a model of cyclic association and dissociation of enzyme from DNA ends during DNA repair. *Biochemistry* **1994**, *33*, 6186−6191.
(53) Rosenthal, D. S.; Ding, R.; Simbulan-Rosenthal, C. M.; Vaillancourt, J. P.; Nicholson, D. W.; Smulson, M. Intact cell evidence for the early synthesis, and subsequent late apopain-mediated suppression, of poly(ADP-ribose) during apoptosis. *Exp. Cell Res.* **1997**, *232*, 313−321.
(54) Kaufmann, S. H.; Desnoyers, S.; Ottaviano, Y.; Davidson, N. E.; Poirier, G. G. Specific proteolytic cleavage of poly(ADP-ribose) polymerase: an early marker of chemotherapy-induced apoptosis. *Cancer Res.* **1993**, *53*, 3976−3985.
(55) Tewari, M.; Quan, L. T.; O'Rourke, K.; Desnoyers, S.; Zeng, Z.; Beidler, D. R.; Poirier, G. G.; Salvesen, G. S.; Dixit, V. M. Yama/CPP32 beta, a mammalian homologue of CED-3, is a CrmA-inhibitable protease that cleaves the death substrate poly(ADP-ribose) polymerase. *Cell* **1995**, *81*, 801−809.
(56) Nicholson, D. W.; Ali, A.; Thornbery, N. A.; Vaillancourt, J. P.; Ding, C. K.; Gallant, M.; Gareau, Y.; Griffin, P. R.; Labelle, M.; Lazebnik, Y. A.; Munday, N. A.; Raju, S. M.; Smulson, M. E.; Yamin, T.-T.; Yu, V. L.; Miller D. K. Identification and inhibition of the ICE/CED-3 protease necessary for mammalian apoptosis. *Nature* **1995**, *376*, 37−43.
(57) Neamati, N.; Fernandez, A.; Wright, S.; Keifer, J.; McConkey, D. J. Degradation of lanim B1 precedes oligonucleosomal DNA fragmentation in apoptotic thymocytes and isolated thymocyte nuclei. *J. Immunol.* **1995**, *154*, 3788−3795.
(58) Buki, K. G.; Bauer, P. I.; Mendeleyev, J.; Hakam, A.; Kun, E. Destabilization of Zn2+ coordination in ADP-ribose transferase (polymerizing) by 6-nitroso-1,2-benzopyrone coincidental with inactivation of the polymerase but not the DNA binding function. *FEBS Lett.* **1991**, *290*, 181−185.
(59) Miller, J.; McLachlan, A. D.; Klug, A. Repetitive zinc-binding domains in the protein transcription factor IIIA from Xenopus oocytes. *EMBO J.* **1985**, *4*, 1609−1614.
(60) Brown, R. S.; Sander, C.; Argos, P. The primary structure of transcription factor TFIIIA has 12 consecutive repeats. *FEBS Lett.* **1985**, *186*, 271−274.
(61) Klug, A. Gene regulatory proteins and their interaction with DNA. *Ann. N.Y. Acad. Sci.* **1995**, *758*, 143−160.
(62) Nelson, H. Structure and function of DNA-binding proteins. *Curr. Opin. Genet. Dev.* **1995**, *5*, 180−189.
(63) Kadonaga, J. K.; Carner, K. R.; Masiarz, F. R.; Tjian, R. Isolation of cDNA encoding transcription factor Sp1 and functional analysis of the DNA binding domain. *Cell* **1987**, *51*, 1079−1090.
(64) Martin, D. I. K.; Orkin, S. H. Transcriptional activation and DNA binding by the erythroid factor GF-1/NF.-E1/Eryf 1. *Genes Dev.* **1990**, *4*, 1886−1898.
(65) Myers, L. C.; Terranova, M. P.; Ferentz, A. E.; Wagner, G.; Verdine, G. L. Repair of DNA methylphosphotriesters through a metalloactivated cysteine nucleophile. *Science* **1993**, *261*, 1164−1167.

JM9708543